Archives of Materials Science and Engineering

Volume 68
Issue 1
July 2014
Pages 10-19

International Scientific Journal
published monthly by the
World Academy of Materials
and Manufacturing Engineering

IR and microscopic studies of polyurethane surface in the Polish extracorporeal ventricular assist device POLVAD-MEV

M. Kościelniak-Ziemniak [a,*], B. Hajduk [b], P. Jarka [c], J. Weszka [b,c], R. Kustosz [a], A. Kapis [a], M. Gonsior [a]

[a] Artificial Heart Laboratory Foundation of Cardiac Surgery Development, Zabrze, Poland
[b] The Centre of Polymer and Carbon Materials PAS,
ul. M. Skłodowskiej-Curie 34, 41-819 Zabrze, Poland
[c] Institute of Engineering Materials and Biomaterials, Silesian University of Technology,
ul. Konarskiego 18a, 44-100 Gliwice, Poland
* Corresponding e-mail address: mkoscielniak_ziemniak@frk.pl

Received 16.04.2014; published in revised form 01.07.2014

ABSTRACT

Purpose: The aim of this article is to show results of IR measurements and microscopic analysis performed on layers prepared with dissolved VAD fragments and pieces of ventricular assist devices cut out of from determined VAD sectors.

Design/methodology/approach: The objects of the study have been POLVAD-MEV VADs from POLCAS system. Four ventricular assist devices POLVAD-MEV have been investigated with use M80 SPECORD IR spectrophotometer and high sensitivity Zeiss – 5 Exciter Confocal Laser Scanning Microscope equipped with a CCD camera.

Findings: The carried IR and microscopic studies showed changes of VAD inner surface. All VAD polyurethane fragments had lower or higher degree of degradation, which isn't directly connected with implantation time.

Research limitations/implications: The polyurethane degradation and surface damage is probably connected with its hydrolysis. The potential effect of blood interaction with VAD inner surface was discussed.

Originality/value: of this paper is spectrophotometer and microscopic studies of polyurethane surface in the polish extracorporeal ventricular assist device POLVAD-MEV.

Keywords: Polyurethane; VAD; POLVAD-MEV; IR spectroscopy; Confocal microscopy

Reference to this paper should be given in the following way:

M. Kościelniak-Ziemniak, B. Hajduk, P. Jarka, J. Weszka, R. Kustosz, A. Kapis, M. Gonsior, IR and microscopic studies of polyurethane surface in the Polish extracorporeal ventricular assist device POLVAD-MEV, Archives of Materials Science and Engineering 68/1 (2014) 10-19.

PROPERTIES

1. Introduction

Polyurethanes (PUs) are the one of the most important groups of the polymers family. They are characterized by excellent mechanical and physical properties as well as high wear resistance [1-2]. Biomedical polyurethanes are also perfectly tolerated by tissues and are characterized by low thrombogenicity. For this reason, they are widely used for medical applications, i.e. ventricular assist devices (VADs) [2].

Urethane elastomers are being obtained from the reactions of diizocyanates with olygomeric diols and low-molecular compounds containing hydroxyl and amino groups [1,3]. Regarding completed medical product polyurethane biodegradation resistance is very important [4,5] Biodegradation is defined as the chemical decomposition of the material being under influence of the biologically active environment impact, leading to the physical properties loss [6,7]. Polymer implant biodegradation in the living organism can proceed on the way of hydrolysis or oxidation processes [8]. Literature data indicate that polyurethane medical products after clinical implantation run a risk of hydrolytic degradation being initialized by the host organism [2]. This phenomena could be dictated of the biological environment pH change, ions and organism enzymes presence [2,9]. The infrared spectroscopy can be used to corroborate the biodegradation of polymeric materials, mainly by monitoring the variation of characteristic bands. In general the structural changes are minimal and a reliable interpretation depends on a right analysis of a set of spectral [6,9].

The objects of the study have been POLVAD-MEV VADs from POLCAS system. Polish heart supporting system – POLCAS, developed in Artificial Heart Laboratory of Religa's Foundation of Cardiac Surgery Development from Zabrze, consists of the extracorporeal heart support device POLVAD and driving unit controlling prosthesis work – POLPDU 401. POLCAS system has been produced since 1999 by Intra-Cordis company and being currently in clinical use in four cardio surgical centres in Poland. Up to now the system has been used in over 290 cases supporting extremely insufficient heart - both like recovery and bridge to transplantation – the longest effective support of patient heart was 680 days.

2. Experimental

Four ventricular assist devices POLVAD-MEV have been investigated. After VADs arrival from clinics and its special preparation processes, they were evaluated in accordance with the inner protocol of Artificial Heart Laboratory. Selected samples of VAD's blood chamber were obtained after human deplantation. The VAD devices were working in connection with patient during different time intervals, the implantation time being equal to 42, 63, 86 and more than 200 days for VAD1, VAD2, VAD3 and VAD4, respectively. The VAD1-3 devices are showed in Figs. 1-3. Eight sectors of inner surface were marked out for every individual VAD.

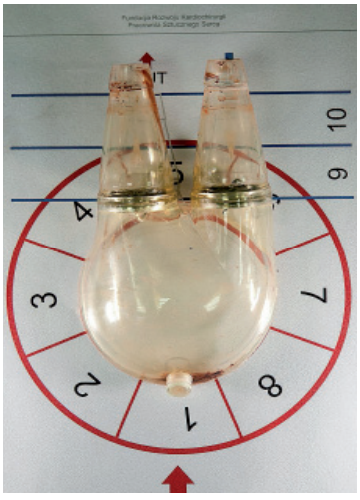

Fig. 1. The adhesion of biological material inside the blood chamber surface of VAD's with implantation time t=42 days

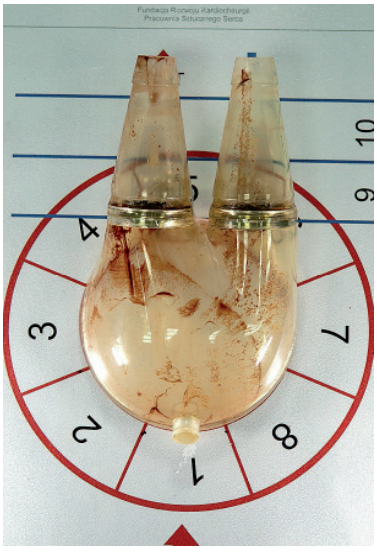

Fig. 2. The adhesion of biological material inside the blood chamber surface of VAD's with implantation time t=63 days

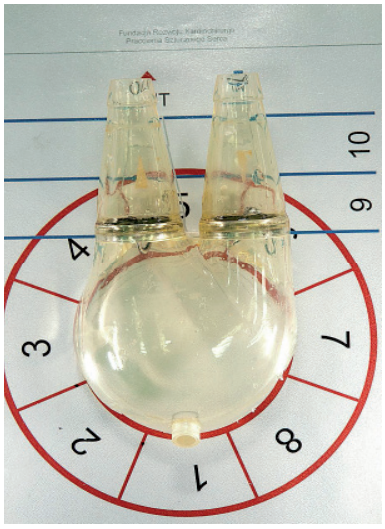

Fig. 3. The adhesion of biological material into the blood chamber surface of VAD's with implantation time t=86 days

Then, polyurethane – DMF solutions were cast onto clean microscopic glass substrates. Prepared samples were dried through 24 hours at temperature lower than 150^0C. Dry thin polyurethane layers were carefully removed from glass surface. Such prepared thin foils of about 1 μm thickness were examined with M80 SPECORD IR spectrophotometer.

The M80 SCPECORD is two-beam spectrophotometer working in 400 – 4000 cm^{-1} wavenumber interval (to 2.5 to 25 μm wavelength).

At the same time fragments cut off from the fourth and eighth sectors were examined with high sensitivity Zeiss 5 Exciter Confocal Laser Scanning Microscope equipped with a CCD camera. Using a confocal microscope enables the imaging in two and three dimensions.

Imaging with laser scanning confocal microscopy allowed accurate representation of damage. Analysis of two-dimensional images allowed to estimate size of defects. In addition, analysis of three-dimensional and topographic images allowed for the depth of defects to be defined.

3. Results

Images of surface morphology taken on cut out inner VAD surface are shown in Figs. 4-11. All images were performed in identical 1.4 x 1.4 mm dimension areas.

Two dimensions images are performed respectively in Figs.4, 6, 8, 10 and three dimensions in Figs. 5, 7, 9, 11.

Pictures taken on surface in the fourth and eighth sectors of VAD2 device are illustrated in Figs. 4-7. The Figs. 8-11 presenting surface morphology in area of the same sectors in VAD4.

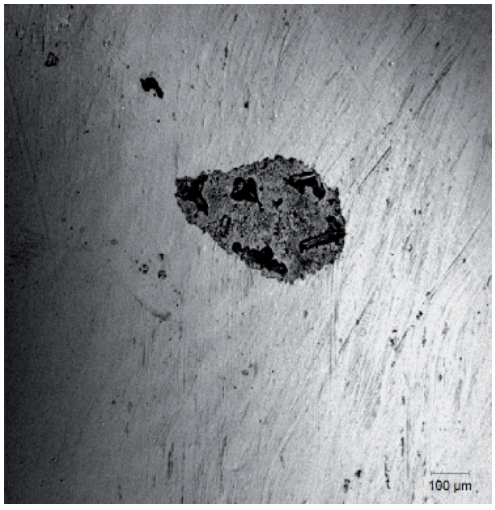

Fig. 4. The 2D microscope image performed with confocal microscope taken on 1.4 x 1.4 mm area in sector 4 of VAD2 device

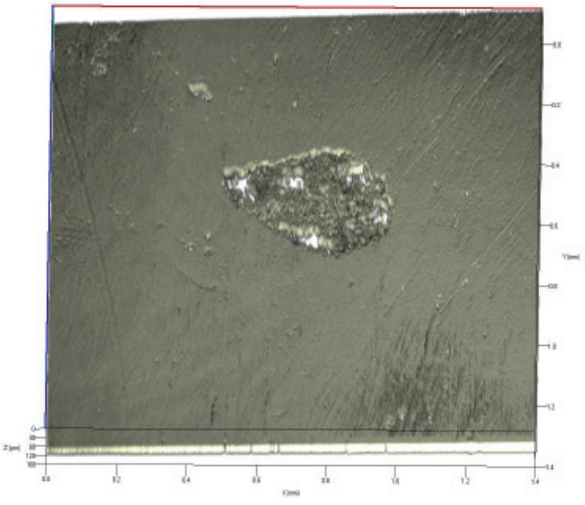

Fig. 5. The 3D microscope image picture performed with confocal microscope taken on 1.4x1.4 mm area in sector 4 of VAD2 device

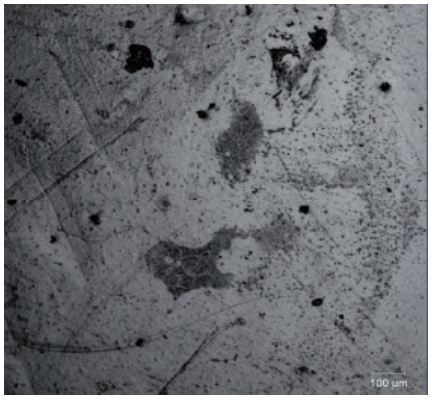

Fig. 6. The picture performed with confocal microscope taken on 1.4x1.4 mm area in sector 8 of VAD2 device

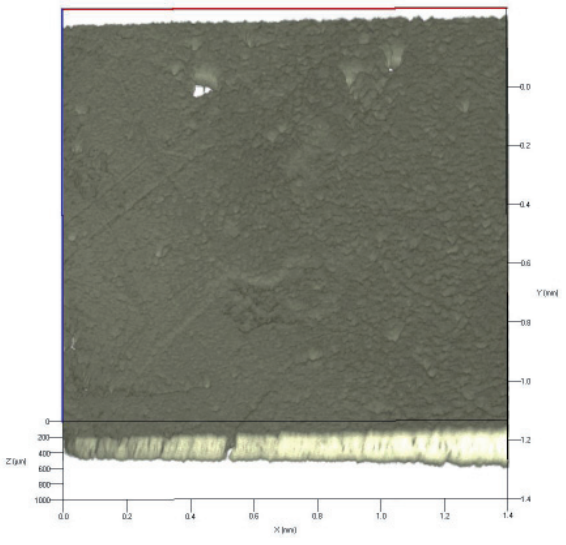

Fig. 7. The picture performed with confocal microscope taken on 1.4x1.4 mm area in sector 8 of VAD2 device

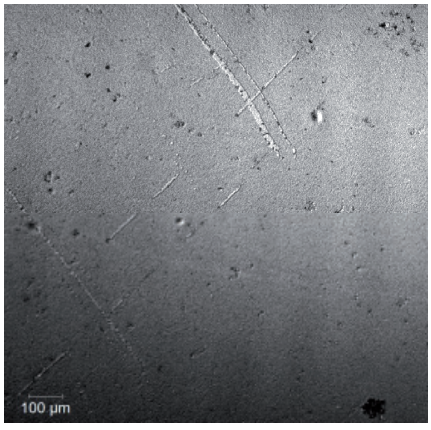

Fig. 8. The 2D microscope image performed with confocal microscope taken on 1.4 x 1.4 mm area in sector 4 of VAD4 device

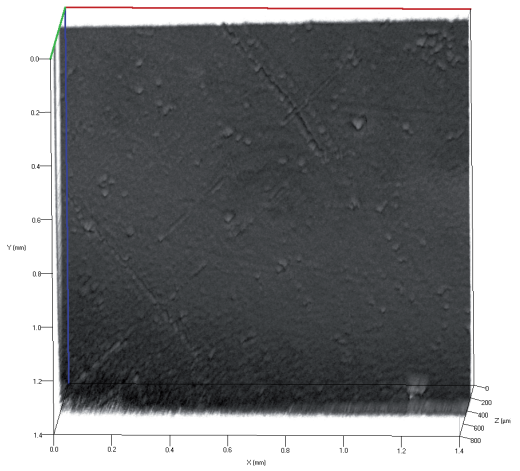

Fig. 9. The picture performed with confocal microscope taken on 1.4x1.4 mm area in sector 8 of VAD4 device

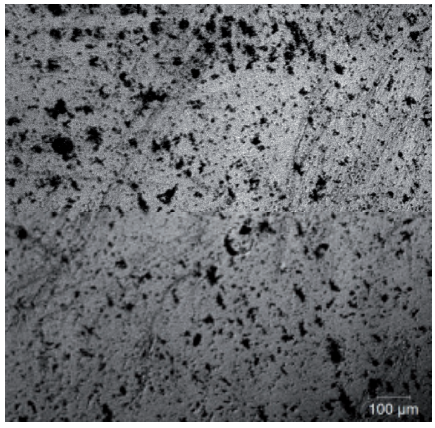

Fig. 10. The 2D microscope image performed with confocal microscope taken on 1.4 x 1.4 mm area in sector 8 of VAD4 device

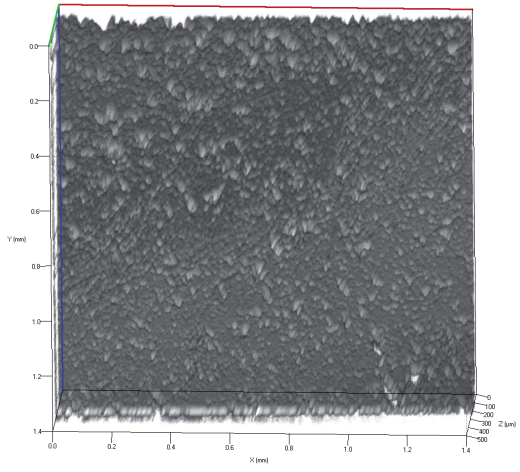

Fig. 11. The picture performed with confocal microscope taken on 1.4x1.4 mm area in sector 8 of VAD4 device

The IR spectra taken on thin foils prepared from the VAD pieces coming from the fourth and eighth sectors of VAD1-4 are shown in Figs 12-15. One can see in all the spectra, that beyond 500-1750 and 2750-3500 cm^{-1} wave number intervals no peaks are seen. The strongest peaks in the first wavenumber interval are grown at about 1116, 1220, 1312, 1532 and 1716 cm^{-1}, the weaker ones are seen at about 1312 and 1412, 1600 cm^{-1} while the weakest peaks are seen at about 660, 772, 820, 1076 and 1364 cm^{-1}. Within the second interval spanning 2750-3500 cm^{-1} range the strongest peaks are at about 2884, 2924 and 3328 cm^{-1}. The weaker peak is seen at about 2800 cm^{-1}.

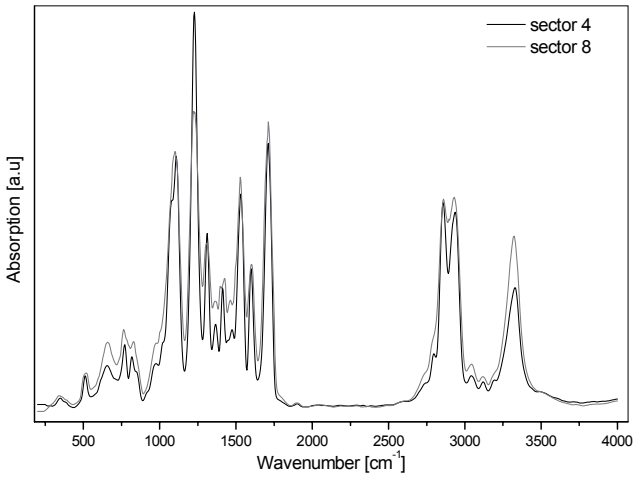

Fig. 12. IR spectrum of aromatic ether-based polyurethane performed on material taken from sector 4 and sector 8 of VAD1 device

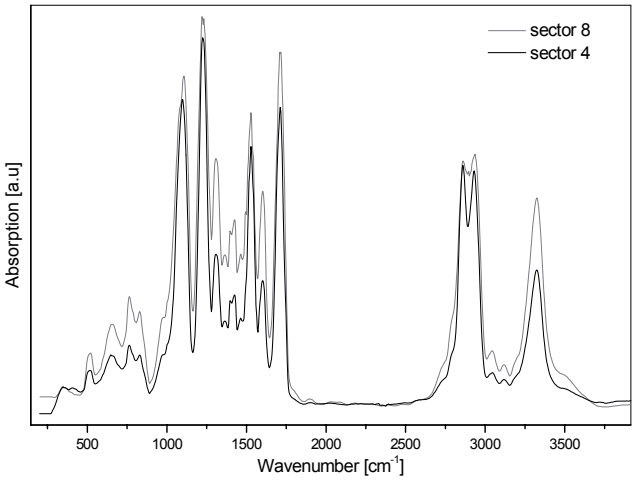

Fig. 13. IR spectrum of aromatic ether-based polyurethane performed on material taken from sector 4 and sector 8 of VAD2 device

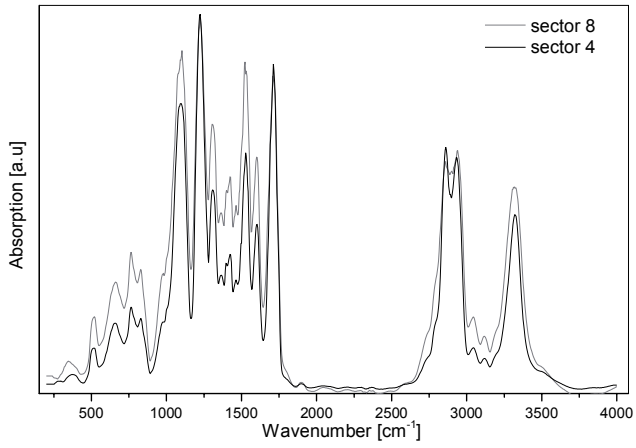

Fig. 14. IR spectrum of aromatic ether-based polyurethane performed on material taken from sector 4 and sector 8 of VAD3 device

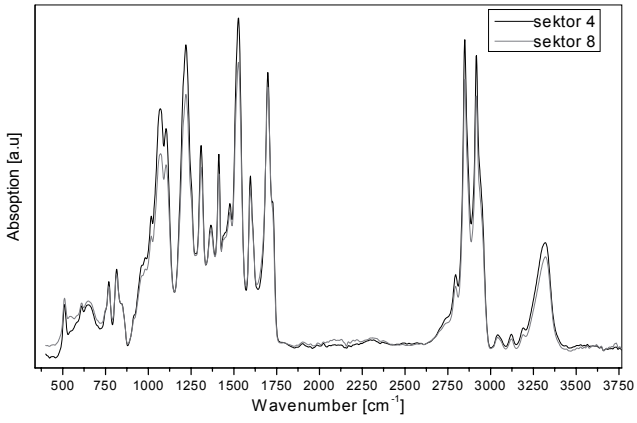

Fig. 15. IR spectrum of aromatic ether-based polyurethane performed on material taken from sector 4 and sector 8 of VAD4 device

4. Discussion

Spectra taken on polyurethane thin foils prepared from materials cut off from the fourth and eighth sectors of all the VAD devices together with the reference spectrum added are showed in Figs. 12-15. The reference spectrum was performed on sample prepared from the same polyurethane material as VAD devices were made of. All the spectra for the reasons mentioned in the previous section were divided into two groups spanning 360-1800 cm^{-1} and 2600-3500 cm^{-1} intervals. The majority of individual peaks can be attributed to characteristic functional groups and their intensity changes is connected with material degradation.

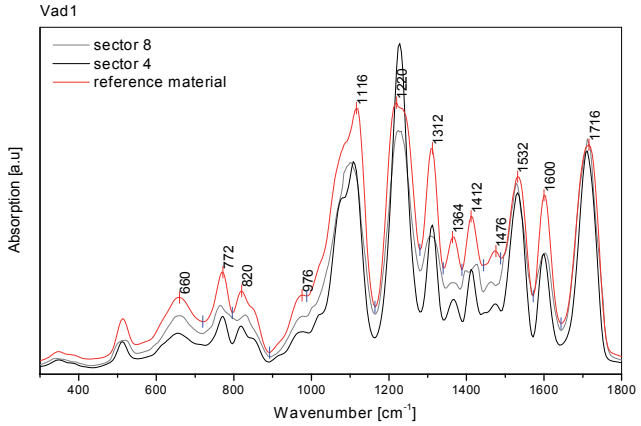

Fig. 16. The IR spectrum taken on samples obtained from VAD1 device in range 300-1800 cm^{-1}

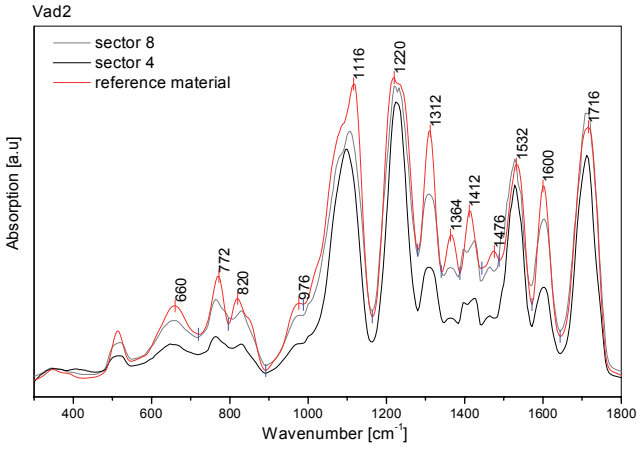

Fig. 17. The IR spectrum taken on samples obtained from VAD2 device in range 300-1800 cm^{-1}

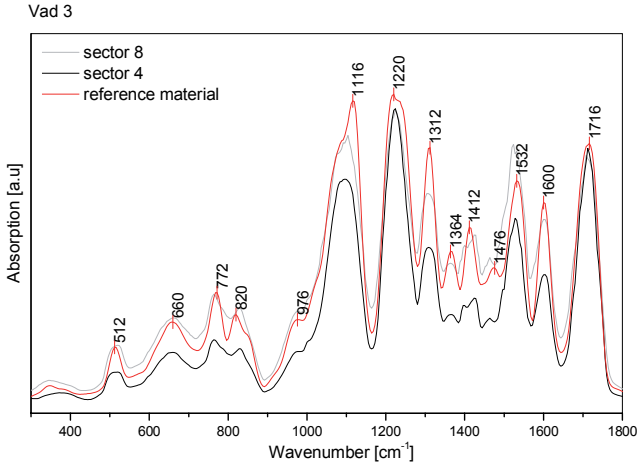

Fig. 18. The IR spectrum taken on samples obtained from VAD3 device in range 300-1800 cm^{-1}

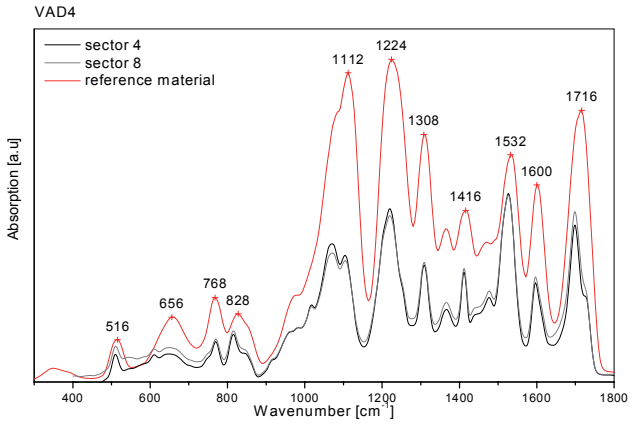

Fig. 19. The IR spectrum taken on samples obtained from VAD1 device in range 300-1800 cm^{-1}

A broad band stretched from 600 cm^{-1} to 800 cm^{-1} wavenumber is due to N-H single bond vibrations and the 772 cm^{-1} frequency is connected with wagging N-H vibrations, while adjacent peak at about 820 cm^{-1} overlapping high frequency wing of the abroad band can be attributed to deformation vibrations of C-H bond contained in CH2 methylene group.

The sharp absorption peak with high intensity placed at about 1116 cm^{-1} is attributed to strong stretching vibration of C-O single bonding located in ether group. From the other hand the peak with strongest absorption intensity is placed at about 1220 cm^{-1} and this vibration is connected with stretching vibration of C-O contained in =C-O-C group, which is characteristic for aromatic ethers. Other strong peak, which absorption has been dramatically decreased (if we compare with reference material spectrum in all cases), placed at about 1312 cm^{-1} results from stretching C-N group vibration. Probably middle peak placed at about 1364 cm^{-1} is connected with wagging vibration of C-H single bonding. Further two weak peaks at about 1412 cm^{-1} and at about 1476 cm^{-1} come from in-plane deforming C-H group vibration and phenylene ring vibration, respectively. The absorption intensity of last three mentioned peaks has been decreased if we compare with reference spectrum.

Strong peak placed at about 1532 cm^{-1} is due to coupling of bending vibration of secondary N-H amine group and stretching vibration of C-N bond, contained in urethane group. The further peak, which intensity also has been decreased is placed at about 1600 cm^{-1}. This frequency is attributed to stretching vibration of C=C groups located in aromatic phenylene rings. The 1716 cm^{-1} peak comes from stretching vibration of C=O carbonyl group. We didn't observe changes of absorption intensity of 1716 cm^{-1} peak in VAD1, VAD3 and VAD4 spectra. The exception here's spectrum of VAD2 where its intensity is little lower.

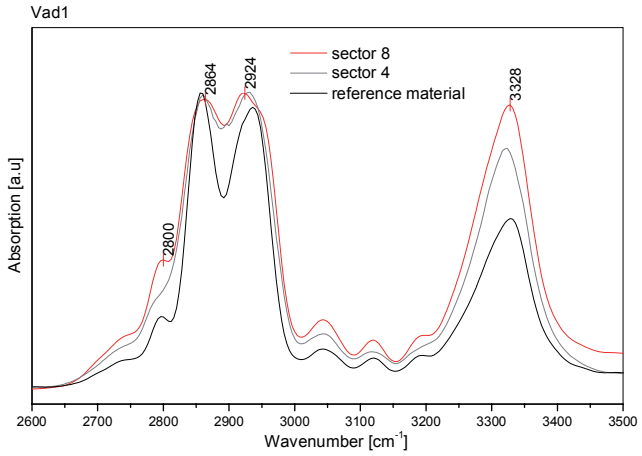

Fig. 20. The IR spectrum taken on samples obtained from VAD1 device in range 2800-3500 cm^{-1}

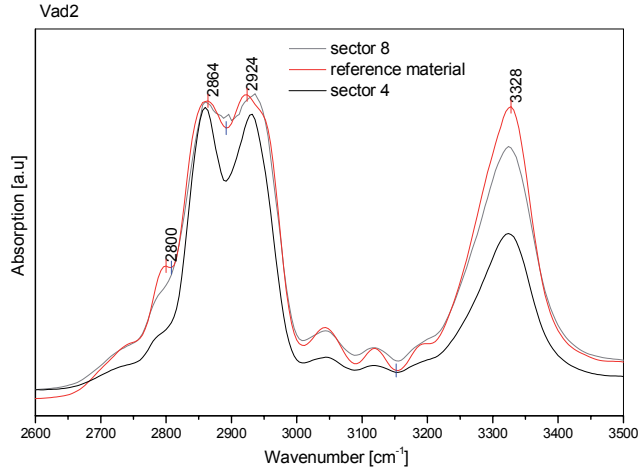

Fig. 21. The IR spectrum taken on samples obtained from VAD2 device in range 2800-3500 cm^{-1}

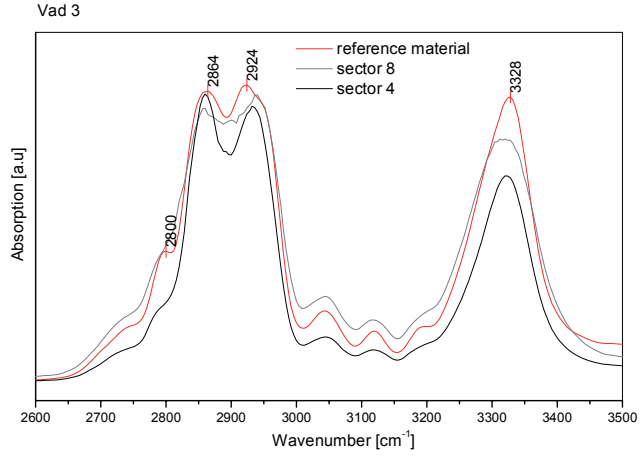

Fig. 22. The IR spectrum taken on samples obtained from VAD3 device in range 2800-3500 cm^{-1}

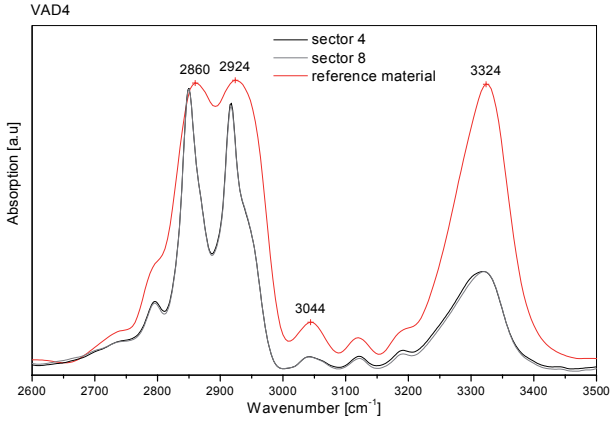

Fig. 23. The IR spectrum taken on samples obtained from VAD4 device in range 2800-3500 cm^{-1}

Two bands, which form doublet are placed at about 2864 cm^{-1} and 2924 cm^{-1}. The first of these peaks is attributed to symmetrical stretching vibration of CH_2 methylene group and the second one is connected with asymmetrical stretching CH_2 vibration. The doublet of methylene group stretching vibration isn't observable in reference material. The last of all mentioned bands is peak placed at about 3328 cm^{-1} connected with secondary amine N-H group stretching vibration. The 2800-2300 cm^{-1} doublet is formed more separated if we compare with reference spectrum in all cases. Just the definitely formed doublet is seen in VAD4 spectrum.

The intensity of a weak abroad band in range 500-900 cm^{-1} has been decreased in all graphs. Also the intensity decrease of 1076, 1116, 1312, 1364, 1412,1532, 1476, 1600 and 3328 cm^{-1} peaks has been observed. The peaks placed at about 1716, 2864 and 2924 cm^{-1} didn't reveal a significant changes of their absorption intensity. A visible increase of peaks absorption is seen in IR spectrum of VAD1 device, showed in Fig. 12.

The intensity of 1120 cm^{-1} peak is higher than intensity of the same peak in reference spectrum and in spectrum taken on sample from sector 8.

Decrease of all peaks intensity is more visible in spectra of VAD4 device and is about 50 % lower if we compare with reference material.

All spectra differences, which were mentioned above are more clearly observed in spectra taken on samples obtained from 4 sectors. Also the intensities decreases are more visible in four sector than in eight sector.

One can see, that intensity of peaks connected with N-H vibration (3328 cm^{-1} and 1312 cm^{-1}) has been decreased in the all graphs, especially in spectra taken on samples from 4 sector if VADs.

The exception is absorption graph of VAD4 device, where the N-H vibration is very low. This fact suggests that the proportion ratio of N-H function groups has been changed. The amount of N-H single bonds in sector 4 is lower than the same one in sector 8 and is comparable for both sectors in VAD4 device. The decrease of 1116 cm^{-1} correspond to breaking of C-O single bonds contained in urethane groups.

All changes observed in recorded spectra suggest aging and chemical degradation of polyurethane applied in VAD's production. The degradation of polymer seems to be caused by interaction of VAD's inner surface with flowing blood ingredients, like oxygen, water and enzymes. Usually the immediate contact of polymer with organic components causes the degradation of material in hydrolysis way. The general scheme of hydrolysis reaction of urethane groups is showed in Figs. 24-25.

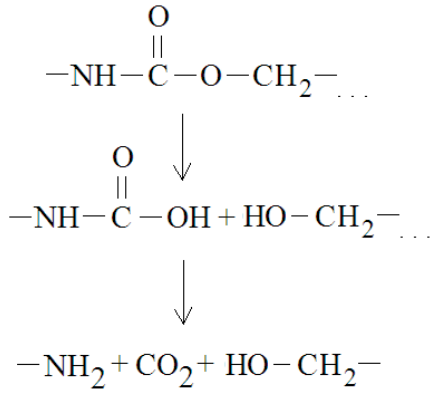

Fig. 24. The general scheme of urethane group hydrolysis

During the hydrolysis of ether group the hydrogen contained in β-methylene group is moved to carbonyl oxygen atom. The α methylene carbon contained in ether group is the carbonium ion, what results in ether $C_\alpha O$ single bonds breaking. The α and β carbon indexes are shown in Fig. 21.

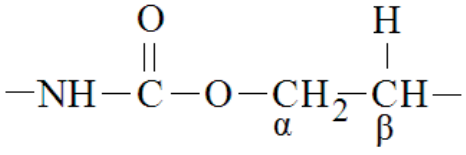

Fig. 25. α and β carbon indexes

The mild surface degradation of VADs was confirmed by microscopic analysis.

The microscopic images taken on 4 and 8 sectors of VAD2 and VAD4 devices are shown in Figs. 4-11. Two and three dimensional pictures of the same area show discontinuities in polyurethane surface. Usually there are linear defects and holes, which are superficial enough. The average length of linear defects is about 1 mm and holes diameter is around 20-200 μm.

It's clearly seen that 1.4x1.4 mm area showed in Fig.10 (VAD4) is more defected than the same dimension area showed in Fig. 6 (VAD2). It's in good accordance with time of contact between urethane surface and human blood, which was longer in VAD4.

The large surface discontinuity of VAD2 which diameter is about two hundred micrometers and its depth is about 50 μm is visible in Fig. 4 (sector 4). The sector 8 of the same device is more damaged with linear defects and mild holes. The average length of linear defects is around 0.5-1mm and average hole's diameter is about 5-50 μm. The maximum value of visible holes depth is about 70 μm.

The similar damages of surface has been showed in Figs.8 and 10, which were performed on VAD4 fragments (sector 4 and 8). The numerous mild holes and a linear defects are visible in presented areas. We found that this kind of damage is more visible in sector 8.

The average diameter of holes visible in sector 4 is about 10 μm and the diameter of the largest one is about 50 μm. The average depth of holes is about 100 μm. The length of linear defects is in range 100-400 μm.

The wide holes are more numerous in sector 8 of VAD4 device than in the same sector of VAD2. Their average diameter is about 10 μm and the diameter of the biggest observed hole is about 80 μm. The length of visible linear defects is in range 100-600 μm.

The linear defects visible in microscopic images are more numerous in sector 4 of both of devices (VAD2 and VAD4). We assume that these kind of surface damage is connected with blood flows inside the devices.

5. Conclusions

Thin polyurethane foils were prepared from VAD1-4 pieces taken from 4 and 8 sectors of every device were checked with IR absorption spectroscopy. Also the fragments cut off from sector 4 and sector 8 of VAD2 and VAD4 were checked with confocal microscopy.

Carried IR investigations showed that C-O-C and N-H peak intensities has been decreased in all obtained spectra.

Also the decrease of these peaks is more visible in spectra taken on polyurethane foils from 4 sectors. These changes indicate breaking of C-O single bonds contained in urethane groups and the decrease of N-H groups amount.

At once the most probably degradation should be connected with hydrolysis of urethane groups. We should note that sector 4 is more subjected for contact with blood ingredients on the ground that coagulums are forming onto its surface.

The degradation which is connected with changes visible in IR spectra don't clearly correspond with time of VADs exploitation. The explanation is fact that VADs were working with individual patients.

The confocal microscopy analysis performed on VAD2 and VAD4 fragments showed that surface is damaged in all checked fragments. The holes and the linear defects are visible in sectors 4 and 8 of VADs. The damaging of surface is more advanced in fragments cut off from VAD4 device.

However comparing the results of confocal microscopy and IR spectroscopic results it can be concluded that observed damages are mechanical and are not a result of VAD's degradation.

Obtained results show that changes of polyurethane material are not very significant for VAD's working time.

Acknowledgements

Examinations were performed in cooperation of Foundation for Cardiosurgery Development and Center of Polymer and Carbon Materials Polish Academy of Science in Zabrze.

References

[1] M. Sobczak, Z. Florjańczyk, E. Dąbek, W. Parasiewicz, Urethane elastomers with polycarbonate soft segments, Elastomers 8/1 (2004) 15-19 (in Polish).

[2] H. Madra, S.B. Tantekin-Ersolma, F.S. Guner, Monitoring of oil-based polyurethane synthesis by FTIR-ATR, Polymer Testing 28 (2009) 773-779.

[3] Y. Zhu, J. Xiong, Y. Tang, Y. Zuo, EIS study on failure process of two polyurethane composite coatings, Progress in Organic Coatings 69/1 (2010) 7-11.

[4] I. Szleifer, Polymers and proteins: interactions at interfaces, Current Opinion in Solid State and Materials Science 2/3 (1997) 337-344.

[5] K. Mequanint, R. Sanderson, Hydrolytic stability of nano-particle polyurethane dispersions: Implications to their long-term use, European Polymer Journal 42/5 (2006) 1145-1153.

[6] J.R. Kloss, T. Hommerding Pedrozo, H. Dal Magro Follmann, P. Peralta-Zamora, J. Alves Dionísio, L. Akcelrud, S.F. Zawadzki, L. Pereira Ramos, Application of the principal component analysis method in the biodegradation polyurethanes evaluation, Materials Science and Engineering C 29 (2009) 470-473.

[7] M. Pechar, A. Braunová, K. Ulbrich, M. Jelínková, B. Øíhová, L. Seymour, Hydrolytically and reductively degradable carriers of biologically active molecules based on multiblock polymers of poly(ethylene glycol), Journal of Controlled Release 116/2 (2006) e8-e10.

[8] D. Sarkar, S.T. Lopina, Oxidative and enzymatic degradations of L-tyrosine based polyurethanes, Polymer Degradation and Stability 92 (2007) 1994-2004.

[9] P.Z. Zhao, Y.S. Wang, J.H. Zhu, X.Y. Hua, Q.Z. Wen, Characterization of graded polyurethane elastomer by FTIR, Science in China Series B: Chemistry 51/1 (2008) 58-61.

[10] E. Orgilés-Calpena, F. Arán-Aís, A.M. Torró-Palau, C. Orgilés-Barceló, J.M. Martín-Martínez, Effect of annealing on the properties of waterborne polyurethane adhesive containing urethane-based thickener, International Journal of Adhesion and Adhesives 29/8 (2009) 774-780.

[11] L.H. Chan-Chan, R. Solis-Correa, R.F. Vargas-Coronado, J.M. Cervantes-Uc, J.V. Cauich-Rodríguez, P. Quintana, P. Bartolo-Pérez, Degradation studies on segmented polyurethanes prepared with HMDI, PCL and different chain extenders, Acta Biomaterialia 6 (2010) 2035-2044.

[12] B. Ravat, M. Grivet, Y. Grohens, A. Chambaudet, Electron irradiation of polyesterurethane: study of chemical and structural modifications using FTIR,

UV spectroscopy and GPC, Radiation Measurements 34 (2001) 31-36.
[13] V. Melnig, L. Obreja, A. Garlea, In vitro degradation and erosion of degradable lactate segmented polyurethanes, Journal of Optoelectronics and Advanced Materials 7/6 (2005) 2803-2808.
[14] B.H. Stuart, Infrared Spectroscopy, Fundamentals and Applications, Wiley, New York, 2004.